PAPER

Stable Fe(III) phenoxyimines as selective and robust CO$_2$/epoxide coupling catalysts†

Eszter Fazekas, [ID] Gary S. Nichol, [ID] Michael P. Shaver [ID] and Jennifer A. Garden [ID] *
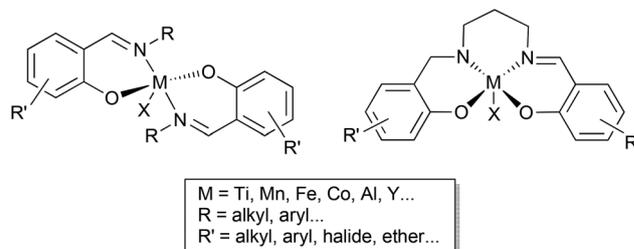
Three phenoxyimine Fe(III)Cl complexes bearing electronically diverse -Cl, -H or -^{t}Bu substituents in the *ortho* position were synthesised. X-ray crystallographic analysis of the complexes reveals mononuclear structures with pentacoordinate iron centres and trigonal bipyramidal geometries. All three complexes demonstrated excellent catalytic activities towards CO$_2$/epoxide coupling to selectively form cyclic carbonates, with catalyst activity correlating with the electron withdrawing nature of the *ortho*-substituent (Cl > H > ^{t}Bu) and thus the Lewis acidity of the metal centre. The chloro-substituted complex displayed remarkable activity in the synthesis of propylene carbonate from propylene oxide and CO$_2$, reaching turnover frequencies (TOF) up to 760 h^{-1} in the presence of TBABr co-catalyst at 120 °C and 20 bars of CO$_2$ pressure. Importantly, the catalyst is also very robust, functioning with high substrate loading, under air or in the presence of water. The substrate scope was successfully extended to other terminal epoxides including epichlorohydrin (TOF = 900 h^{-1}) and to the more challenging internal epoxide, cyclohexene oxide (TOF = 80 h^{-1}). These are amongst the highest TOF values reported for an iron CO$_2$/epoxide coupling catalyst to date.

Introduction

Catalytic transformations of carbon dioxide (CO$_2$) are an important strategy to valorise this waste gas and potentially reduce the environmental impact of its accumulation in the atmosphere. Epoxide coupling is an effective and atom efficient method to use this inexpensive, renewable C1 building block. Depending on the catalyst system and the reaction conditions used, polycarbonates and/or cyclic carbonates are formed; the latter are applied as high boiling solvents, ion-carriers for batteries, reagents for lignin functionalisation, fuel additives and precursors to polymer synthesis.[1–6] The key to CO$_2$/epoxide coupling is to combine high selectivity with high activity, as the synthesis of both cyclic carbonates and polycarbonates requires the catalyst system to overcome the significant activation energy barrier of these transformations.[1,7,8]

Some of the most active catalyst systems comprise homogeneous complexes with a Lewis acidic metal centre

(for epoxide coordination and activation) and a nucleophile (for ring opening of the epoxide). Ligand design has enabled the development of highly efficient catalyst systems, including mono- or bi-metallic ligand supported complexes with ammonium or phosphonium salt co-catalysts, or bifunctional catalysts which incorporate the onium salt into the ligand backbone.[9–12] One popular ligand framework is the privileged salen ligand scaffold, which has supported many Lewis acidic complexes mediating a wide array of small and large molecule transformations (Scheme 1).[13–15] While the ubiquitous salen ligands have shown some success in CO$_2$/epoxide coupling, their bidentate phenoxyimine (half salen) analogues have been underexplored.[16] Breaking the bridge between the phenoxy

*EaStCHEM School of Chemistry, University of Edinburgh, Edinburgh, EH9 3FJ, UK.
E-mail: j.garden@ed.ac.uk*

†Electronic supplementary information (ESI) available: ^{1}H and ^{13}C NMR spectra and single crystal X-ray diffraction data. CCDC 1855808–1855810. For ESI and crystallographic data in CIF or other electronic format see DOI: 10.1039/c8dt02919a

Scheme 1 General structure of a bis(phenoxyimine) complex *vs.* a salen complex.

M = Ti, Mn, Fe, Co, Al, Y...
R = alkyl, aryl...
R' = alkyl, aryl, halide, ether...

groups creates a more flexible coordination environment, enabling the balance between the steric hindrance and the accessibility of the metal centre to be better fine-tuned (Scheme 1). Previous findings in the field suggest that the coordination mode of the metal centre is a key feature in allowing the efficient conversion of sterically challenging internal epoxides to cyclic carbonates.[1]

We have had a longstanding interest in iron-mediated catalysis thanks to its abundance, low cost, and low toxicity.[17,18] In particular, Fe^{3+} compounds offer a user-friendly route into catalysis, due to their air- and moisture-stability which enables convenient synthesis and handling. Only a few examples of mono- or bi-metallic $Fe(III)$ complexes have been reported as catalysts for CO_2/epoxide couplings and in most cases high catalyst loadings were required to achieve good conversions.[16,19–27] Uniting these joint ligand and metal benefits, we targeted a series of phenoxyimine $Fe(III)$ chloride complexes as robust and flexible catalysts for epoxide/CO_2 coupling.

Results and discussion

Three phenoxyimine ligand precursors were targeted, bearing *ortho*-substituents of H (**L1**, Scheme 2), ^tBu (**L2**) or Cl (**L3**). Accordingly, all three ligands were synthesised in excellent yields (95–99%) *via* the straightforward condensation of methyl amine and mono-substituted salicylaldehydes (Scheme 2).[28] Confirming the synthesis of **L1**, **L2** and **L3**, no aldehyde resonances were present in the ^1H NMR spectra, and diagnostic imine resonances were observed (CDCl₃ solvent, **L1**, $\delta = 8.33$; **L2**, $\delta = 8.35$; **L3**, $\delta = 8.30$). Complexes **C1**–**C3** were synthesised through deprotonation of pro-ligands **L1**–**L3** using NaH (1.1 eq.) to form the corresponding Na-phenolates. Subsequent reaction with anhydrous $FeCl_3$ (0.5 eq.) in THF solvent at room temperature gave an immediate colour change from yellow to dark purple, which indicated the formation of the bis-ligated $Fe(III)$ chloride complexes **C1**–**C3**. After purification *via* filtration to remove residual NaCl, the products were isolated in high yields (74–98%, Scheme 2) as dark purple/brown solids. As the paramagnetically shifted ^1H NMR spectra of **C1**–**C3** provided limited information, the stoichiometry was confirmed *via* high resolution mass spectrometry and elemental analysis.

The complexes proved to be oxygen- and moisture-stable, and single crystals suitable for X-ray diffraction were obtained under air. Crystals of complexes **C1** and **C3** were obtained *via* the slow evaporation of DCM, while crystals of **C2** were obtained *via* the slow evaporation of toluene. Single crystal X-ray diffraction studies revealed that all three complexes have a mononuclear structure, with a pentacoordinate $Fe(III)$ centre displaying a slightly distorted trigonal bipyramidal (TBP) geometry. In each case, the TBP character is high, as established using the factors of equatorial TBP (TBP_e: **C1** ≥ 99.9%; **C2** ≥ 99.9%; **C3** ≥ 99.9%) and axial TBP (TBP_a: **C1** ≥ 99.9%; **C2** = 97.7%; **C3** = 99.8%) proposed by Tamao and Ito (Fig. 1–3).[29] For all three complexes, the axial N–Fe–N bond angle deviates slightly from linearity (N–Fe–N, **C1**, 177.44(5)°; **C2**, 169.7(2)°; **C3**, 174.92(7)°), while the sum of the equatorial O–Fe–Cl and O–Fe–O bond angles is 360° (**C1**, 360.00°; **C2**, 360.01°; **C3**, 360.01°). The steric bulk of the *ortho*-substituents notably influences the distortion of the TBP geometry at the Fe centre, with the sterically demanding ^tBu group leading to the greatest deviation from linearity for the N–Fe–N bond angle, and the lowest TBP_a character. These 'half salen' frameworks significantly differ from $Fe(III)$ salen complexes,[30] as the phenoxyimine ligands are arranged such that both nitrogen and both oxygen atoms are in mutually *trans* positions. This difference in geometry arises from the lack of a bridge connecting the
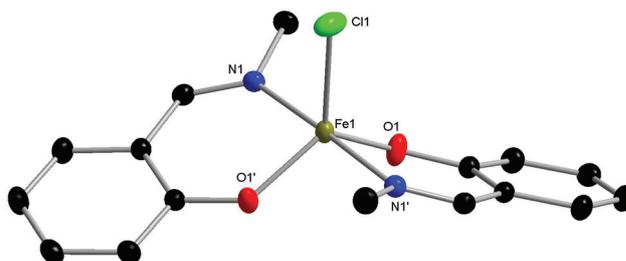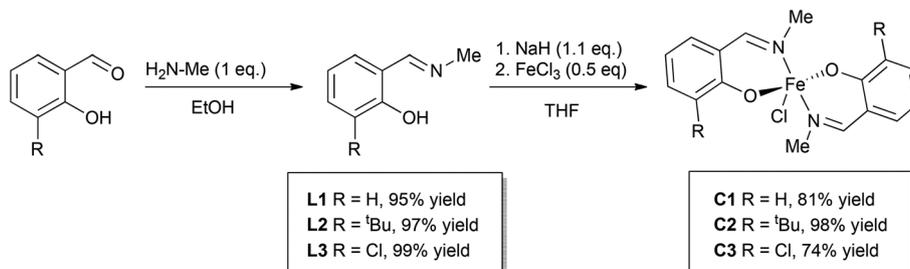

Fig. 1 Molecular structure of **C1** with ellipsoids set at the 50% probability level. Hydrogen atoms have been omitted for clarity. Selected bond lengths (Å): Fe1–Cl1 2.2713(5), Fe1–O1 1.8758(9), Fe1–O1′ 1.8757 (9), Fe1–N1 2.111(1), Fe1–N1′ 2.111(1). Selected bond angles (°): O1–Fe1–Cl1 119.50(3), O1′–Fe1–Cl1 119.50(3), O1′–Fe1–O1 121.00(6), O1′–Fe1–N1′ 90.29(4), O1–Fe1–N1′ 88.46(4), O1–Fe1–N1 90.28(4), O1′–Fe1–N1 88.46(4), N1′–Fe1–Cl1 91.28(3), N1–Fe1–Cl1 91.28(3), N1–Fe1–N1′ 177.44(5).

Scheme 2 Synthesis of pro-ligands **L1**–**L3** and $Fe(III)$ phenoxyimine complexes **C1**–**C3**.

L1 R = H, 95% yield
L2 R = ^tBu, 97% yield
L3 R = Cl, 99% yield

C1 R = H, 81% yield
C2 R = ^tBu, 98% yield
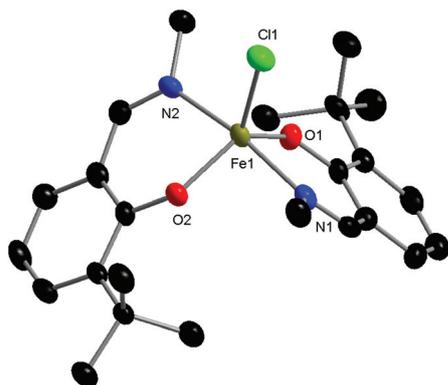**C3** R = Cl, 74% yield

Fig. 2 Molecular structure of **C2** with ellipsoids set at the 50% probability level. Hydrogen atoms and co-crystallised solvent have been omitted for clarity. Selected bond lengths (Å): Fe1–Cl1 2.245(2), Fe1–O1 1.880(5), Fe1–O2 1.881(4), Fe1–N1 2.103(6), Fe1–N2 2.108(6). Selected bond angles (°): O1–Fe1–Cl1 116.1(2), O2–Fe1–Cl1 119.4(2), O2–Fe1–O1 124.6(2), N1–Fe1–Cl1 93.6(2), N1–Fe1–O1 87.5(2), N1–Fe1–O2 87.5(2), N2–Fe1–Cl1 96.8(2), N2–Fe1–O1 88.5(2), N2–Fe1–O2 86.9(2), N2–Fe1–N1 169.7(2).
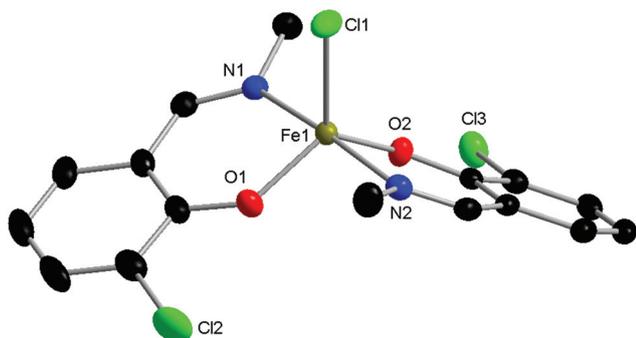

Fig. 3 Molecular structure of **C3** with ellipsoids set at the 50% probability level. Hydrogen atoms have been omitted for clarity. Selected bond lengths (Å): Fe1–Cl1 2.2517(6), Fe1–O1 1.871(2), Fe1–N1 2.092(2), Fe1–O2 1.889(2), Fe1–N2 2.104(2). Selected bond angles (°): O1–Fe1–N1 88.64(7), O1–Fe1–Cl1 117.12(5), O1–Fe1–O2 121.78(7), O1–Fe1–N2 89.43(7), N1–Fe1–Cl1 92.25(5), N1–Fe1–N2 174.92(7), O2–Fe1–N1 89.00(7), O2–Fe1–Cl1 121.11(5), O2–Fe1–N2 88.02(7), N2–Fe1–Cl1 92.81(5).

two phenoxy groups, enabling the phenoxyimine ligands to minimise the steric repulsion of the substituted imine ligands. These complexes bear similar structural motifs to those observed with related phenoxyimine Fe(III)–chloride complexes, including those with bulky substituents on the imine groups.[16,31–37] The bond metrics are comparable to reported examples of structurally characterised phenoxyimine Fe(III) complexes,[16] with Fe–N bond lengths ranging from 2.092(2) to 2.111(1) Å and Fe–O bond lengths ranging from 1.8757(9) to 1.889(2) Å.[33,34,38]

The C–O bond lengths of complexes **C1**, **C2** and **C3** are short [1.328(1) Å, 1.318(8) Å and 1.321(3) Å, respectively] in comparison to the related protonated ligand bearing a naphthalene substituent on the imine N [C–O, 1.354(2) Å].[39]

These short C–O bonds are indicative of resonance delocalisation of the anionic charge on the phenoxide ligand in complexes **C1–C3**. Furthermore, the C–C bond lengths of the (O–)C=C–C(=N) scaffold within **C1–C3** lie between the expected bond lengths for $C_{(aromatic)}=C_{(aromatic)}$ double bonds and $C_{(aromatic)}-C$ single bonds (1.40 and 1.52 Å, respectively),[40] suggestive of resonance delocalisation through the phenoxyimine moiety. This resonance delocalisation is most pronounced for the electron donating ^{t}Bu-substituted complex **C2** [C1–C6, 1.434(9); C6–C7, 1.43(1) Å], followed by the unsubstituted CH analogue **C1** [C1–C6, 1.417(2); C6–C7, 1.447(2) Å] and the electron withdrawing Cl analogue **C3** [C1–C6, 1.411(3); C6–C7, 1.450(3) Å].

To test the catalytic activity of complexes **C1–C3** towards CO_2/epoxide coupling, propylene oxide (PO) was selected as a benchmark substrate, as it has previously been studied with other iron catalysts.[16] Initially, complex **C2** was tested under solvent free conditions using 0.1 mol% catalyst loading with 0.1 mol% tetrabutylammonium iodide (TBAI) as a co-catalyst (*vs.* PO), using 20 bar pressure of CO_2 at 120 °C. ^{1}H and ^{13}C NMR studies of the crude mixture revealed that the catalysts were selective towards the formation of cyclic propylene carbonate (Fig. S8†).[41] Under these conditions, **C2** successfully achieved 99% conversion to cyclic propylene carbonate in 12 hours (Table 1, entry 2). Control reactions testing only the Fe-complex **C2** (entry 4) or only co-catalyst TBAI (entry 5) showed that both components individually display low activity, however, their combination displayed a synergistic effect with a significantly higher conversion achieved (*cf.* entries 1 and 3). A systematic optimisation of the reaction conditions was subsequently performed. Catalyst **C2** displayed tolerance towards an increased substrate loading of 1 : 2000 ([Fe] : [PO]), reaching a high TOF value of 400 h^{-1} (Table 1, entry 6). Doubling the co-catalyst ratio from 1 to 2 equivalents (*vs.* catalyst **C2**) further improved the turnover frequency of the catalyst system, from 400 h^{-1} to 480 h^{-1} (Table 1, entries 6 and 8, respectively). Finally, tetrabutylammonium bromide (TBABr) was investigated as a co-catalyst, which resulted in a modest improvement in the catalytic activity (entry 12, TOF = 510 h^{-1}). Kinetic studies were performed and confirmed a linear, first-order relationship between substrate conversion and time, highlighting the catalyst stability under the reaction conditions tested (Fig. 4). All three Fe(III) phenoxyimine complexes were subsequently screened for CO_2/PO coupling using the optimised reaction conditions (Table 1, entries 11–13).

The reactivity trends fall in line with the electron withdrawing/donating ability of the *ortho*-substituent, with the electron withdrawing Cl group (**C3**) giving the highest catalytic activity (TOF = 760 h^{-1}, entry 13), followed by the *ortho*-H analogue **C1** (TOF = 530 h^{-1}, entry 11) and the electron donating ^{t}Bu substituent **C2** (TOF = 510 h^{-1}, entry 12). Comparing **C1–C3** to other Fe(III) catalysts known for this transformation is rather complex due to the range of different conditions used, as shown by specific catalytic comparators provided in the ESI (Table S2†). However, the high catalytic activity of *ortho*-chloro-substituted **C3** is particularly notable, as it is amongst the

Table 1 Synthesis of propylene carbonate from CO_2 and propylene oxide catalysed by complexes **C1–C3**

$$\text{PO} \xrightarrow[\text{120°C, 20 bar}]{\substack{CO_2 \\ \text{[Fe]/ co-cat}}} \text{propylene carbonate}$$

Entry	Complex	t (h)	[PO]/[Fe]	Co-cat.	[Co-cat]/[Fe]	Conv. (%)	TON	TOF (h^{-1})
1	**C2**	24	1000	TBAI	1	99	990	41
2	**C2**	12	1000	TBAI	1	99	990	83
3	**C2**	2	1000	TBAI	1	56	560	280
4	**C2**	24	1000	—	0	13	130	5
5[a]	—	2	1000	TBAI	2	15	—	—
6	**C2**	2	2000	TBAI	1	40	800	400
7	**C2**	2	1000	TBAI	2	91	910	455
8	**C2**	2	2000	TBAI	2	48	960	480
9	**C1**	2	2000	TBAI	2	48	960	480
10	**C3**	2	2000	TBAI	2	69	1380	690
11	**C1**	2	2000	TBABr	2	53	1060	530
12	**C2**	2	2000	TBABr	2	51	1020	510
13	**C3**	2	2000	TBABr	2	76	1520	760
14[b]	**C3**	2	2000	TBABr	2	43	860	430
15[c]	**C3**	2	2000	TBABr	2	65	1300	650
16	**C3**	2	10 000	TBABr	2	11	1100	550
17	**C3**	26	10 000	TBABr	2	63	6300	242
18[d]	**C3**	24	10 000	TBABr	2	51	5100	213

Conditions: 100 ml stainless steel autoclaves, 20 bar CO_2 pressure, 120 °C, neat. Conversion was determined using ^1H NMR spectra of crude reaction mixtures. [a] The reaction was carried out without an iron complex, 2 equivalents of TBAI were added per 1000 equivalents of epoxide. [b] 100 equivalents H_2O/[Fe] was added. [c] The reaction was carried out under air. [d] The reaction was carried out using unpurified propylene oxide (99%).
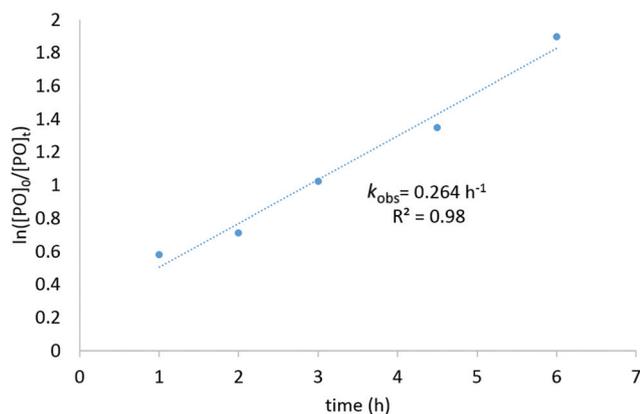
Fig. 4 Kinetic plot for the synthesis of propylene carbonate using **C2** with 2000 equivalents of substrate.

fastest reported Fe-based catalyst systems for cyclic carbonate formation. It seems likely that the presence of electron withdrawing chloro- groups increases the Lewis acidity of the Fe centre, facilitating epoxide coordination to promote nucleophilic attack and ring-opening.[42] These findings conform to previous studies of cobalt(III) amidoamine ligands, which showed a similar trend; complexes bearing electron withdrawing chloro- or nitro- substituents gave significantly enhanced catalyst activities in comparison to the methyl substituted analogues.[43]
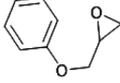
In addition to their high catalytic activity, it is particularly noteworthy that **C1**, **C2** and **C3** are all air-stable complexes.

When the coupling reaction was set up under air, *ortho*-chloro catalyst **C3** still displayed high activities towards cyclic propylene carbonate formation, with only a minor reduction in the TOF value observed (entry 13, TOF = 760 h^{-1}; entry 15, TOF = 650 h^{-1}). Furthermore, catalyst system **C3** also displayed some tolerance towards water; the addition of 100 equivalents of water (*vs.* catalyst **C3**) still gave high TOF values of 430 h^{-1} (entry 14). Catalyst **C3** is noteworthy as it demonstrates high catalytic activities even at low catalyst loadings of 0.01 mol% (1 : 10 000 [Fe] : [PO]), displaying a TOF of up to 550 h^{-1} after 2 hours (entry 16), slowing only after 8 hours (Fig. S12†). The robustness of **C3** was further demonstrated when high conversion was maintained using 10 000 equivalents of unpurified (wet) PO (entry 18). The water tolerance of catalyst **C3** was supported by FT-IR spectroscopic studies (refer to ESI† for further details).

The substrate scope of catalyst **C3** towards CO_2/epoxide coupling was investigated by testing a range of epoxides, including cyclohexene oxide (CHO), epichlorohydrin, 1,2-epoxybutane and 1,2-epoxy-3-phenoxypropane (Table 2). Catalyst **C3** demonstrated tolerance towards a broad substrate scope, successfully converting all five substrates tested to the corresponding cyclic carbonates. For the terminal epoxides, the catalyst activity falls in line with the nature of the epoxide substituent, with the presence of electron withdrawing substituents facilitating the epoxide ring opening. Accordingly, the highest conversion was observed for epichlorohydrin (TOF = 900 h^{-1}, Table 2, entry 3), and the lowest conversion (of a terminal epoxide) was achieved for butylene oxide (TOF = 500 h^{-1}, entry 4). In agreement with previously observed trends,[1] the

Table 2 Substrate scope for CO_2/epoxide coupling using catalyst **C3**
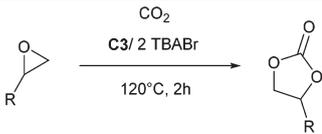
Entry	Substrate	Substrate loading	Conv. (%)	TON	TOF (h^{-1})
1		2000	76	1520	760
2		2000	8	160	80
3		2000	90	1800	900
4		2000	50	1000	500
5		1500	69	1035	518

Conditions: 100 ml stainless steel autoclaves, 20 bar CO_2 pressure, 120 °C, 2 hours, neat. Conversion was determined using ^{1}H NMR spectra of crude reaction mixtures.

lowest conversions were observed for the most sterically hindered internal epoxide, cyclohexene oxide, as expected due to the formation of a strained bicyclic carbonate product. Through extending the reaction time to 48 hours, high conversion of CHO to cyclohexene carbonate (CHC) was achieved (74%, Table S1,† entry 3). This is indeed surprising, as catalysts which selectively give CHC in high yields are still rare, as many catalyst systems yield a mixture of poly(cyclohexene carbonate) (PCHC) and CHC.[1,20,44,45] Importantly, catalyst **C3** exclusively formed *cis*-CHC at high conversions, which is quite unusual as the formation of the *trans*-isomer often occurs through the thermodynamically favourable back-biting of a poly(cyclohexene carbonate) chain. However, resonances corresponding to *trans*-CHC (3.9 ppm) were absent from the ^{1}H NMR spectra, and IR spectroscopy and mass spectrometry (EI and MALDI) studies of the product mixture confirmed the lack of polymer formation (Fig. S13–15†).[1,20] The formation of *cis*-CHC occurs through a double inversion pathway, which can be favoured through the addition of excess co-catalyst.[20,46–50]

It has previously been proposed that the metal geometry is of key importance for the conversion of sterically congested internal epoxides to the corresponding cyclic carbonates, with complexes bearing a trigonal bipyramidal geometry around the metal centre typically showing greater success.[1,51] Complexes **C1–C3** all display a distorted trigonal bipyramidal geometry, in contrast to the square pyramidal geometries often observed

with Fe(III) salen complexes.[52–55] The flexible coordination modes available when using phenoxyimine ligands may present an advantage over the well-established salen analogues. These findings suggest that phenoxyimine ligand supported metal complexes have significant potential for a broad scope of CO_2/epoxide coupling reactions.

Conclusions

In conclusion, three new iron(III) phenoxyimine complexes were synthesised and tested in CO_2/epoxide coupling reactions. All three earth-abundant, air-tolerant complexes display excellent performance in the selective catalytic coupling of CO_2/epoxides, when activated by the presence of a tetrabutylammonium bromide or iodide co-catalyst. These results highlight that for this class of catalysts, the activity is influenced by the presence of electron donating or electron withdrawing *ortho*-substituents on the phenoxyimine ligand. The highest catalyst activities were achieved using the electron withdrawing chloro-substituted complex **C3**, with TOF values up to 900 h^{-1}. Importantly, the complexes are very robust, tolerating the presence of both air and water, and very flexible, selectively forming the *cis* isomer of cyclohexene carbonate from the sterically challenging secondary epoxide. These iron catalyst precursors offer significant potential as stable, robust and selective catalysts for the valorisation of carbon dioxide.

Experimental

General procedure for ligand precursors L1–L3

Equimolar amounts of a salicylaldehyde (salicylaldehyde, 3-*tert*-butylsalicylaldehyde or 3-chlorosalicylaldehyde) and methylamine (40% w/w solution in water) were dissolved in ethanol (0.2 M) and stirred at room temperature for 16 hours. The resulting yellow solutions were dried over $MgSO_4$, filtered, and the solvents were subsequently evaporated *in vacuo*. **L1** was obtained as an orange oil, whilst **L2** and **L3** were further purified *via* recrystallisation from ethanol, to produce **L2** as green crystals and **L3** as yellow crystals. Characterisation data for **L1** was in agreement with reported values in the literature.[56]

Data for L2: (1.86 g, 97%) ^{1}H NMR (500 MHz, CDCl$_3$) δ 14.11 (s, 1H, O*H*), 8.35 (s, 1H, *H*C=N), 7.31 (d, J = 7.7 Hz, 1H, Ar*H*), 7.10 (d, J = 7.6 Hz, 1H, Ar*H*), 6.80 (t, J = 7.6 Hz, 1H, Ar*H*), 3.48 (d, J = 1.5 Hz, 3H, NC*H*$_3$), 1.44 (s, 9H, CC*H*$_3$). ^{13}C NMR (126 MHz, CDCl$_3$) δ 166.89 (*C*=N), 160.51 (*C*-OH), 137.43, 129.32, 129.13, 118.75, 117.63 (Ar-*C*), 45.72 (N-*C*H$_3$), 34.83 (*C*CH$_3$), 29.32 (C*C*H$_3$). HRMS (EI): m/z [M]$^+$ 191.1319 calculated [M]$^+$ 191.1310.

Data for L3: (1.10 g, 99%) ^{1}H NMR (500 MHz, CDCl$_3$) δ 14.51 (s, 1H, O*H*), 8.29 (s, 1H, *H*C=N), 7.39 (d, J = 7.9 Hz, 1H, Ar*H*), 7.14 (d, J = 7.7 Hz, 1H, Ar*H*), 6.77 (t, J = 7.8 Hz, 1H, Ar*H*), 3.49 (d, J = 1.5 Hz, 3H, C*H*$_3$). ^{13}C NMR (126 MHz, CDCl$_3$) δ 165.8 (*C*=N), 158.8 (*C*-OH), 132.7, 129.6, 122.2, 119.3, 118.1 (Ar-*C*) 44.9 (*C*H$_3$). HRMS (EI): m/z [M]$^+$ 169.0315 calculated [M]$^+$ 169.0294.

General procedure for complexes C1–C3

To a solution of pro-ligand (**L1**–**L3**) in THF, 1.1 equivalents of NaH was gradually added and the mixture was stirred at ambient temperature for 1 hour. A solution of anhydrous $FeCl_3$ (0.5 eq.) in THF was added dropwise to afford a dark coloured mixture that was stirred for a further 16 hours at room temperature. Solvents were evaporated *in vacuo* and the crude product was taken up in toluene. The NaCl by-product was removed by filtration through Celite and the filtrate was dried *in vacuo*. The crude products were washed three times with hexane to afford dark purple-brown powders. Single crystals suitable for X-ray diffraction analysis were obtained *via* slow evaporation of DCM or toluene.

Data for C1 (0.42 g, 81%) HRMS (EI): m/z $[M]^+$ 359.0205 calculated $[M]^+$ 359.0250 elemental analysis calculated for $C_{16}H_{16}ClFeN_2O_2$: C, 53.4; H, 4.5; N, 7.8. Found: C, 53.3; H, 4.65; N, 7.6.

Data for C2 (2.11 g, 98%) HRMS (EI): m/z $[M]^+$ 471.1523 calculated $[M]^+$ 471.1502 elemental analysis calculated for $C_{24}H_{32}FeN_2O_2$: C, 61.1; H, 6.84; N, 5.9. Found: C, 60.2; H, 6.2; N, 6.0.

Data for C3 (0.49 g, 74%) HRMS (EI): m/z $[M]^+$ 426.9474 calculated $[M]^+$ 426.9475 elemental analysis calculated for $C_{16}H_{14}Cl_3FeN_2O_2$: C, 44.85; H, 3.3; N, 6.5. Found: C, 44.7; H, 3.35; N, 6.5.

General procedure for the synthesis of cyclic carbonates from CO_2 and epoxides

Reactions were carried out in 100 mL stainless steel autoclaves equipped with a magnetic stirrer, heating mantle (controlled by a thermocouple) and a pressure gauge. Complex **C1**, **C2** or **C3** (10.0 μmol) and co-catalyst (TBAI or TBABr) were placed into the autoclave and purged with argon. The relevant epoxide (2000 eq.) was added and the autoclave was subsequently pressurised with 20 bar of CO_2. The autoclave was heated to 120 °C for 24 hours, then rapidly cooled in an ice bath for 1 hour and slowly vented. An aliquot of the crude reaction mixture was immediately taken up in $CDCl_3$ and analysed *via* ^1H NMR spectroscopy, to determine epoxide conversion *via* integration of product resonances against starting material resonances (refer to ESI† for further details).

Crystallography

Single crystal X-ray diffraction data were collected on an Rigaku Oxford Diffraction SuperNova diffractometer fitted with an Atlas CCD detector with Mo-Kα radiation ($\lambda = 0.7107$ Å) or Cu-Kα radiation ($\lambda = 1.5418$ Å). Crystals were mounted under Paratone on MiTeGen loops. The structures were solved by direct methods using SHELXS or SHELXT and refined by full-matrix least-squares on F^2 using SHELXL interfaced through Olex2.[57,58] Molecular graphics for all structures were generated using Diamond.

Conflicts of interest

There are no conflicts of interest to declare.

Acknowledgements

References

1 C. Martín, G. Fiorani and A. W. Kleij, *ACS Catal.*, 2015, **5**, 1353–1370.

2 H. Büttner, L. Longwitz, J. Steinbauer, C. Wulf and T. Werner, *Top. Curr. Chem.*, 2017, **375**, 50.

3 D. C. Webster and A. L. Crain, *Prog. Org. Coat.*, 2000, **40**, 275–282.

4 H. Zhang, H.-B. Liu and J.-M. Yue, *Chem. Rev.*, 2014, **114**, 883–898.

5 B. Schäffner, F. Schäffner, S. P. Verevkin and A. Börner, *Chem. Rev.*, 2010, **110**, 4554–4581.

6 A. Duval and L. Avérous, *ACS Sustainable Chem. Eng.*, 2017, **5**, 7334–7343.

7 H. Sun and D. Zhang, *J. Phys. Chem. A*, 2007, **111**, 8036–8043.

8 C.-H. Guo, H.-S. Wu, X.-M. Zhang, J.-Y. Song and X. Zhang, *J. Phys. Chem. A*, 2009, **113**, 6710–6723.

9 M. Chihiro, T. Tomoya, O. Kanae and E. Tadashi, *Angew. Chem., Int. Ed.*, 2015, **54**, 134–138.

10 C. J. Whiteoak, N. Kielland, V. Laserna, F. Castro-Gomez, E. Martin, E. C. Escudero-Adan, C. Bo and A. W. Kleij, *Chemistry*, 2014, **20**, 2264–2275.

11 H. Vignesh Babu and K. Muralidharan, *Dalton Trans.*, 2013, **42**, 1238–1248.

12 J. Qin, P. Wang, Q. Li, Y. Zhang, D. Yuan and Y. Yao, *Chem. Commun.*, 2014, **50**, 10952–10955.

13 P. G. Cozzi, *Chem. Soc. Rev.*, 2004, **33**, 410–421.

14 A. W. Kleij, *Eur. J. Inorg. Chem.*, 2009, 193–205.

15 J. A. Castro-Osma, M. North and X. Wu, *Chem. – Eur. J.*, 2016, **22**, 2011–2017.

16 F. A. Al-Qaisi, N. Genjang, M. Nieger and T. Repo, *Inorg. Chim. Acta*, 2016, **442**, 81–85.

17 K. Zhu, M. P. Shaver and S. P. Thomas, *Chem. Sci.*, 2016, **7**, 3031–3035.

18 K. Zhu, J. Dunne, M. P. Shaver and S. P. Thomas, *ACS Catal.*, 2017, **7**, 2353–2356.

19 K. Nakano, K. Kobayashi, T. Ohkawara, H. Imoto and K. Nozaki, *J. Am. Chem. Soc.*, 2013, **135**, 8456–8459.

20 A. Buchard, M. R. Kember, K. G. Sandeman and C. K. Williams, *Chem. Commun.*, 2011, **47**, 212–214.

21 C. J. Whiteoak, B. Gjoka, E. Martin, M. M. Belmonte, E. C. Escudero-Adán, C. Zonta, G. Licini and A. W. Kleij, *Inorg. Chem.*, 2012, **51**, 10639–10649.

22 M. A. Fuchs, T. A. Zevaco, E. Ember, O. Walter, I. Held, E. Dinjus and M. Doring, *Dalton Trans.*, 2013, **42**, 5322–5329.

23 A. Buonerba, A. De Nisi, A. Grassi, S. Milione, C. Capacchione, S. Vagin and B. Rieger, *Catal. Sci. Technol.*, 2015, **5**, 118–123.

24 M. İkiz, E. İspir, E. Aytar, M. Ulusoy, Ş. Karabuğa, M. Aslantaş and Ö. Çelik, *New J. Chem.*, 2015, **39**, 7786–7796.

25 C. J. Whiteoak, E. Martin, E. Escudero-Adán and A. W. Kleij, *Adv. Synth. Catal.*, 2013, **355**, 2233–2239.

26 F. Della Monica, S. V. C. Vummaleti, A. Buonerba, A. D. Nisi, M. Monari, S. Milione, A. Grassi, L. Cavallo and C. Capacchione, *Adv. Synth. Catal.*, 2016, **358**, 3231–3243.

27 F. Della Monica, B. Maity, T. Pehl, A. Buonerba, A. De Nisi, M. Monari, A. Grassi, B. Rieger, L. Cavallo and C. Capacchione, *ACS Catal.*, 2018, **8**, 6882–6893.

28 F. M. García-Valle, R. Estivill, C. Gallegos, T. Cuenca, M. E. G. Mosquera, V. Tabernero and J. Cano, *Organometallics*, 2015, **34**, 477–487.

29 K. Tamao, T. Hayashi, Y. Ito and M. Shiro, *Organometallics*, 1992, **11**, 2099–2114.

30 R. Duan, C. Hu, X. Li, X. Pang, Z. Sun, X. Chen and X. Wang, *Macromolecules*, 2017, 9188–9195.

31 J. E. Davies and B. M. Gatehouse, *Acta Crystallogr., Sect. B: Struct. Crystallogr. Cryst. Chem.*, 1972, **28**, 3641–3645.

32 C. J. Magurany and C. E. Strouse, *Inorg. Chem.*, 1982, **21**, 2348–2350.

33 J. M. Becker, J. Barker, G. J. Clarkson, R. van Gorkum, G. K. Johal, R. I. Walton and P. Scott, *Dalton Trans.*, 2010, **39**, 2309–2326.

34 M. Amini, M. M. Haghdoost, M. Bagherzadeh, A. Ellern and L. Keith Woo, *Polyhedron*, 2013, **61**, 94–98.

35 Y. Elerman and H. Paulus, *Acta Crystallogr., Sect. C: Cryst. Struct. Commun.*, 1996, **52**, 1971–1973.

36 M. Amini, A. Arab, P. G. Derakhshandeh, M. Bagherzadeh, A. Ellern and L. K. Woo, *Spectrochim. Acta, Part A*, 2014, **133**, 432–438.

37 A. Mojtaba, B. Mina, D.-H. Sepideh, E. Arkady and W. L. Keith, *Z. Anorg. Allg. Chem.*, 2014, **640**, 385–389.

38 J. A. Bertrand, J. L. Breece and P. G. Eller, *Inorg. Chem.*, 1974, **13**, 125–131.

39 R. Jamjah, M. Nekoomanesh, R. Zahedi, G. Zohuri, F. Afshar Taromi and B. Notash, *Acta Crystallogr., Sect. E: Struct. Rep. Online*, 2012, **68**, 522.

40 G. S. Manku, *Theoretical principles of inorganic chemistry*, Tata McGraw-Hill, New Delhi, 1980.

41 L. Hongchun and N. Yongsheng, *Polym. Adv. Technol.*, 2016, **27**, 1191–1194.

42 D. R. Moore, M. Cheng, E. B. Lobkovsky and G. W. Coates, *J. Am. Chem. Soc.*, 2003, **125**, 11911–11924.

43 P. Ramidi, N. Gerasimchuk, Y. Gartia, C. M. Felton and A. Ghosh, *Dalton Trans.*, 2013, **42**, 13151–13160.

44 D. J. Darensbourg and A. D. Yeung, *Macromolecules*, 2013, **46**, 83–95.

45 M. Taherimehr, S. M. Al-Amsyar, C. J. Whiteoak, A. W. Kleij and P. P. Pescarmona, *Green Chem.*, 2013, **15**, 3083–3090.

46 V. Laserna, G. Fiorani, C. J. Whiteoak, E. Martin, E. Escudero-Adán and A. W. Kleij, *Angew. Chem., Int. Ed.*, 2014, **53**, 10416–10419.

47 J. Langanke, L. Greiner and W. Leitner, *Green Chem.*, 2013, **15**, 1173–1182.

48 C. J. Whiteoak, E. Martin, E. Escudero-Adán and A. W. Kleij, *Adv. Synth. Catal.*, 2013, **355**, 2233–2239.

49 F. Castro-Gómez, G. Salassa, A. W. Kleij and C. Bo, *Chem. – Eur. J.*, 2013, **19**, 6289–6298.

50 D. J. Darensbourg, *Chem. Rev.*, 2007, **107**, 2388–2410.

51 C. J. Whiteoak, N. Kielland, V. Laserna, E. C. Escudero-Adán, E. Martin and A. W. Kleij, *J. Am. Chem. Soc.*, 2013, **135**, 1228–1231.

52 L. D. Wickramasinghe, S. Mazumder, K. K. Kpogo, R. J. Staples, H. B. Schlegel and C. N. Verani, *Chem. – Eur. J.*, 2016, **22**, 10786–10790.

53 Z. Chu, W. Huang, L. Wang and S. Gou, *Polyhedron*, 2008, **27**, 1079–1092.

54 A. Karahan, R. Kurtaran, Y. Yahsi, E. Gungor and H. Kara, *J. Struct. Chem.*, 2016, **57**, 731–736.

55 B. Chen, D. S. Contreras, Y. L. Clancy and F. R. Fronczek, *Acta Crystallogr., Sect. E: Struct. Rep. Online*, 2004, **60**, 732–734.

56 P. A. Nikitina, A. S. Peregudov, T. Y. Koldaeva, L. G. Kuz'mina, E. I. Adiulin, I. I. Tkach and V. P. Perevalov, *Tetrahedron*, 2015, **71**, 5217–5228.

57 G. M. Sheldrick, *Acta Crystallogr., Sect. C: Struct. Chem.*, 2015, **71**, 3–8.

58 O. V. Dolomanov, L. J. Bourhis, R. J. Gildea, J. A. K. Howard and H. Puschmann, *J. Appl. Crystallogr.*, 2009, **42**, 339–341.